1.E.4 *Nuclear Physics* A246 (1975) 231–245;

RECOIL-DISTANCE LIFETIME MEASUREMENTS OF LOW-LYING STATES OF ^{21}Ne, ^{24}Na, ^{25}Mg AND ^{42}K WITH THE B+^{16}O AND ^{26}Mg+^{18}O REACTIONS

H. H. EGGENHUISEN, L. P. EKSTRÖM †, G. A. P. ENGELBERTINK,
J. MONDRIA, M. A. VAN DRIEL and J. A. J. HERMANS
Fysisch Laboratorium, Rijksuniversiteit, Utrecht, The Netherlands

Received 7 April 1975

Abstract: The recoil-distance method has been used in conjunction with the B+^{16}O and ^{26}Mg+^{18}O reactions to measure mean lives of low-lying states of ^{21}Ne, ^{24}Na, ^{25}Mg and ^{42}K. The following results are obtained: ^{21}Ne, $E_x = 0.35$ MeV, $\tau_m = 12.9 \pm 1.6$ ps; ^{24}Na, 0.56 MeV, 46 ± 6 ps; ^{25}Mg, 0.97 MeV, 16.9 ± 1.0 ps; ^{42}K, 0.11 MeV, 410 ± 60 ps; 0.26 MeV, 192 ± 13 ps; 0.70 MeV, 59 ± 11 ps and 1.38 MeV, 1690 ± 120 ps. Excitation energies and branching ratios for ^{42}K levels are given. Combination of γ-γ coincidences on 2 ns delayed γ-rays and the recoil-distance data establish a hitherto unobserved ^{42}K level at an excitation energy of 1375.5 ± 0.2 keV. This level, which decays exclusively to the 699 keV, $J^\pi = (5)^-$ level, is tentatively assigned the stretched isospin configuration $[(1d_{\frac{3}{2}}^{-2})_{0^+1}(1f_{\frac{7}{2}}^{4})_{6^+,1}]_{6^+,2}$. A calculation with a weak-coupling model supports this assignment.

E NUCLEAR REACTIONS ^{10}B(^{16}O, 2pγ), (^{16}O, p$\alpha\gamma$), ^{11}B(^{16}O, pnγ), $E = 24$ MeV; measured recoil-distance. ^{21}Ne, ^{24}Na, ^{25}Mg levels deduced $T_{\frac{1}{2}}$, transition strengths. ^{26}Mg(^{18}O, pnγ), $E = 25$ MeV; measured $\gamma\gamma$ (t), recoil-distance. ^{42}K deduced levels, $T_{\frac{1}{2}}$, transition strengths, δ. Natural B target, enriched ^{26}Mg target. Ge(Li) detectors.

1. Introduction

The use of the recoil-distance (RD) method in fusion-evaporation reactions for lifetime measurements of levels in sd and fp shell nuclei is very fruitful [1–3]).

Investigation of high-spin states, preferentially populated in this type of reactions, often involves lifetimes in the picosecond region. The inherent large recoil velocity of $\beta \approx 3\,\%$ encountered in heavy-ion reactions together with the present day plunger technology makes the measurement of lifetimes in the order of a few picoseconds with the RD technique possible. Another advantage of the high recoil velocity is the possibility to apply the RD technique to γ-rays of rather low energy because the energy splitting due to the Doppler effect is proportional to βE_γ.

The present work reports on RD lifetime measurements for levels of ^{21}Ne, ^{24}Na, ^{25}Mg and ^{42}K, which decay by γ-rays in the 90–700 keV region. The investigation of the ^{24}Na and ^{42}K levels is difficult with conventional reactions.

A newly observed, long-lived state in ^{42}K is studied in detail.

† University of Lund, Lund, Sweden.

2. The ^{16}O bombardment of B

The 0.56 MeV level of ^{24}Na is populated in the $^{10}B(^{16}O, 2p\gamma)^{24}Na$ reaction and the lifetime of this level is measured using the RD technique. At the same time results are obtained for ^{25}Mg(0.97 MeV) and ^{21}Ne(0.35 MeV).

2.1. EXPERIMENTAL DETAILS

With the plunger apparatus [2]) used in the present work the distance between target and stopper can be varied from 0 to 10 cm, with an accuracy of better than 5 μm for the range 0–1000 μm. The target consisted of about 100 $\mu g/cm^2$ natural CB_4 evaporated on a 1 μm thick Ni foil, which was stretched mechanically. The energy of the ^{16}O ions after passage through the Ni foil was 24 MeV. The γ-rays were observed at 0° by means of a 100 cm^3 Ge(Li) detector, placed at 6.7 cm from the target. The stopper, consisting of a 0.3 mm thick Cu layer on a 4 mm thick Al disk, has a transmission of 76 % for 100 keV γ-rays.

2.2. ANALYSIS AND RESULTS

The exponential decay curve of the stopped peak, as a function of the recoil distance D, is given by

$$R(D) \equiv I_0/(I_0+I_s) = \exp(-D/D_m), \tag{1}$$

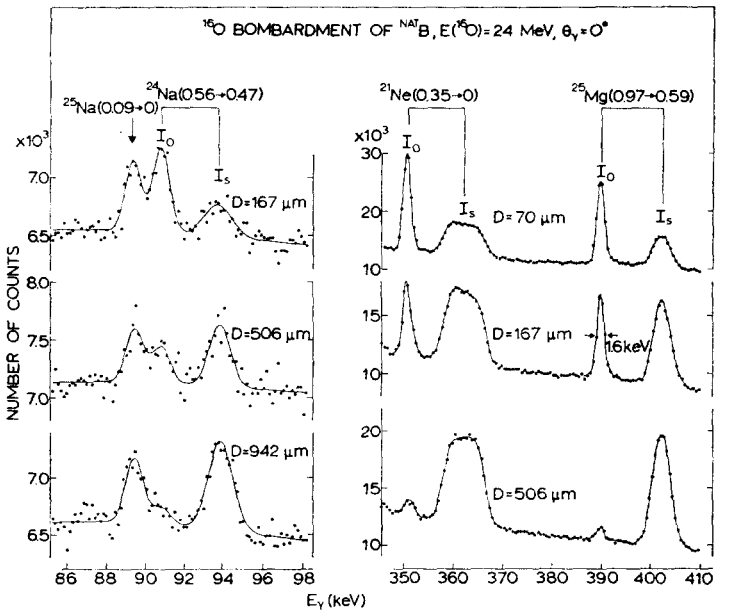

Fig. 1. Examples of the recoil-distance data obtained from ^{16}O bombardment of natural B at different plunger distances D. The line drawn through the data points of the triplet to the left is a fit of three Gaussians on a quadratic background.

where I_0 and I_s are the intensities of the stopped and shifted peaks, respectively. With the mean velocity $\bar{v} = \beta c$ obtained from the observed energy difference between stopped and shifted peak, the mean life τ_m follows from the characteristic distance $D_m = \bar{v}\tau_m$. In extracting the decay curves from the data the intensity of the shifted peak is corrected for the energy dependence of the detector efficiency and the velocity dependence of the solid angle subtended by the detector. The details of this procedure are described in ref. [2]).

A sample of the data from which the mean lives are obtained in the present experiment is shown in fig. 1.

2.2.1. Results for ^{24}Na(0.56 MeV). The 0.56 MeV 2^+ level of ^{24}Na decays (97.5±0.5) % with a 91 keV γ-ray to the 0.47 MeV 1^+ level [4]). The stopped peak of this γ-ray is not completely separated from the 90 keV γ-ray of ^{25}Na(0.09 → 0 MeV) (see fig. 1). The 7.3±0.7 ns mean life [5]) of ^{25}Na(0.09 MeV) ensures that at D = 3 mm still 96 % of the total intensity of the 90 keV γ-ray is in the stopped peak. In the ratio $(I_0^{91}+I^{90})/(I_0^{91}+I_s^{91}+I^{90})$ shown in fig. 2 the intensity of the 90 keV stopped peak I^{90} is therefore considered to be constant. The point at D = 0 μm is inferred from the zero-distance found in fitting the decay curve of the ^{25}Mg(0.97 → 0.59 MeV) transition (see subsect. 2.2.2).

A fit of $\exp(-D/D_m)$+constant to these data yields $D_m = 440\pm60$ μm. The ratio $I_0^{91}/(I_0^{91}+I_s^{91})$ was also determined, by fitting Gaussian lineshapes to the 90, 91_0 and 91_s peaks. This analysis gives $D_m = 450\pm60$ μm. The adopted value of $D_m = 440\pm60$ μm yields with $\beta = (3.20\pm0.05)$ % the mean life $\tau_m = 46\pm6$ ps given in table 1.

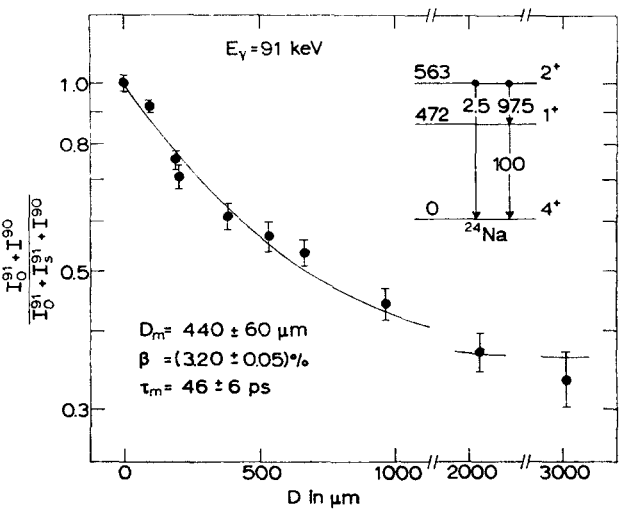

Fig. 2. The experimental ratio $(I_0^{91}+I^{90})/(I_0^{91}+I_s^{91}+I^{90})$ (see subsect. 2.2.1) as a function of target-stopper distance D for the 563 → 472 keV transition in ^{24}Na. The contaminant 90 keV transition stems from the decay of the long-lived (7.3±0.7 ns) first excited state in ^{25}Na. The solid line is a fit of $\exp(-D/D_m)$+constant to the points.

TABLE 1

Recoil-distance lifetime results from ^{16}O bombardment of natural B

Nucleus	E_x (MeV)	Transition (MeV)	τ_m (ps) present	τ_m (ps) previous	Ref.
^{21}Ne	0.35	0.35 → 0	12.9±1.6	22.5±1.0	[8]
				24±5	[10]
				16±4	[9]
				3.6±1.0	[7]
^{24}Na	0.56	0.56 → 0.47	46±6	< 500	[11]
^{25}Mg	0.97	0.97 → 0.59	16.9±1.0	6±4	[8]
				14.6±1.5	[12]
				16±4	[13]

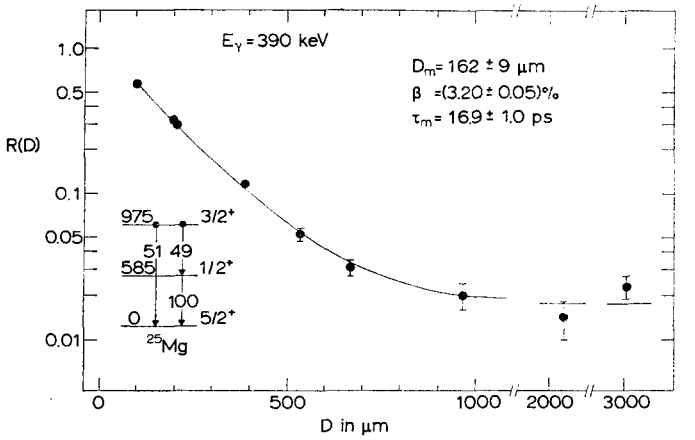

Fig. 3. The experimental ratio $R(D)$ as a function of target-stopper distance D for the 975 → 585 keV transition in ^{25}Mg. The solid line is a fit of $\exp(-D/D_m)$+constant to the points.

The previously known [5]) upper limit of $\tau_m < 500$ ps is consistent with the present result.

2.2.2. The results for ^{25}Mg(0.97 MeV). This level, populated in the $^{11}B(^{16}O, pn\gamma)$ ^{25}Mg reaction, decays (49±2) % to the 0.59 MeV level with a 390 keV γ-ray [5]). The (51±2) % branch to the ground state of ^{25}Mg is, outside the energy range of the spectra in the present experiment. The decay curve of the 390 keV transition is shown in fig. 3. The constant contribution to the stopped peak that shows up at larger distances is due to the β^- decay of ^{25}Na to ^{25}Mg. The half-life of this decay is 59.6 s and the branch to the 0.97 MeV ^{25}Mg level is 27.2 % [ref. [5])]. A fit of $\exp(-D/D_m)$+ constant leads to the lifetime given in table 1.

2.2.3. The results for ^{21}Ne(0.35 MeV). This level is populated in the $^{10}B(^{16}O, \alpha p\gamma)$ ^{21}Ne reaction. Due to the mass of the outgoing particles the ^{21}Ne recoils have a velocity distribution of an appreciable width, as can be seen in fig. 1. The effect of this velocity distribution is taken into account by applying a correction factor $1/\psi$ to the

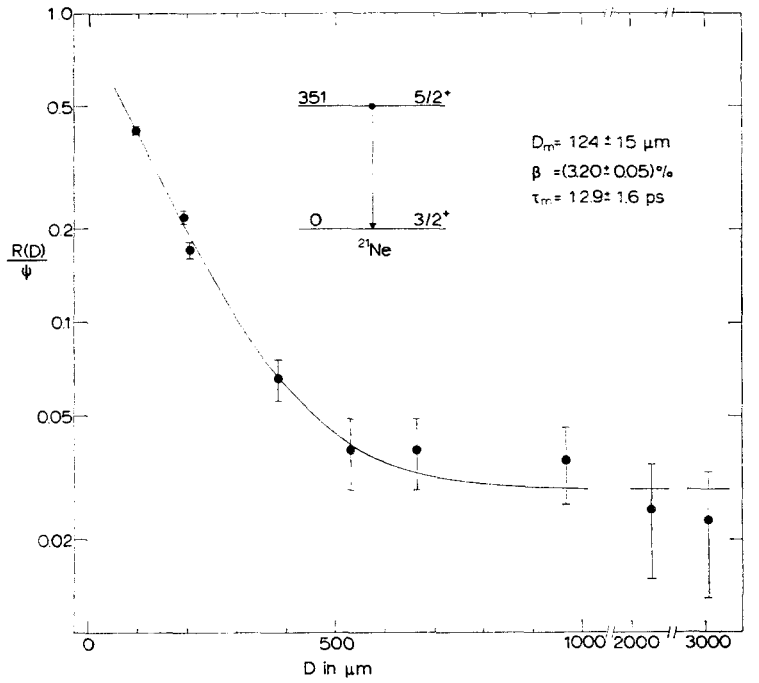

Fig. 4. The experimental ratio $R(D)/\psi$ as a function of the target-stopper distance D for the 351 → 0 keV transition in ^{21}Ne. The quantity ψ is the velocity-distribution correction function, see subsect. 2.2.3. The solid line is a fit of $\exp(-D/D_m)$+constant to the points.

experimental ratios $R(D)$. The expansion of the correction function ψ in terms of the moments of the velocity distribution is given in ref. [2]). The corrected ratios $R(D)/\psi$ are shown in fig. 4. The small constant background, about 3 % of the total intensity of the 351 keV transition, is presumably due to the β-decay of ^{21}F and/or ^{21}Na.

The fit shown in fig. 4 corresponds to a lifetime of 12.9 ± 1.6 ps. Neglect of the velocity distribution would result in a 3 % larger value. The present result disagrees with the values of 3.6 ± 1.0 ps from a DSA measurement [7]) and 22.5 ± 1.0 ps obtained in a recoil-distance experiment [8]). The error in the latter result seems, in view of the data, to be underestimated. The present result is in good agreement with the value of 16 ± 4 ps from ref. [9]) (see table 1).

3. The ^{18}O bombardment of ^{26}Mg

3.1. RECOIL DISTANCE LIFETIME MEASUREMENTS FOR ^{42}K LEVELS

The ^{42}K levels at $E_x = 0.11, 0.26$ and 0.70 MeV are populated in the ^{26}Mg (^{18}O, pnγ)^{42}K reaction. Decay curves of γ-rays de-exciting these levels and also of a 677 keV γ-ray have been measured. In subsect. 3.2 the 677 keV γ-ray is shown to originate from a hitherto unobserved ^{42}K level at $E_x = 1375.5 \pm 0.2$ keV.

3.1.1. Experimental method and results. The target consisted of a 100 μg/cm^2 layer ^{26}Mg (enriched to 99.4 %) evaporated on the downstream side of a 1 μm thick stretched Ni foil. The energy of the ^{18}O ions was 25 MeV after passage through the Ni foil. This energy was chosen to optimize the ratio between the 106.78 $\pm$ 0.02 keV γ-ray of ^{42}K(0.11 $\rightarrow$ 0 MeV) and the 105.89 $\pm$ 0.02 keV γ-ray of ^{38}Ar(4.59 $\rightarrow$ 4.48 MeV). The latter is produced in the competing ^{26}Mg(^{18}O, α2nγ)^{38}Ar reaction. The ratio of the intensities of the 107 and 106 keV γ-rays is about 1 at $E(^{18}\text{O}) = 30$ MeV and 10 at $E(^{18}\text{O}) = 25$ MeV. Spectra were recorded at target-stopper distances between 30 μm and 2 cm with a 100 cm^3 Ge(Li) detector at $\theta_\gamma = 0°$ and at a distance of 6 cm from the target. A sample of the data is shown in fig. 5.

The variation of the solid angle subtended by the Ge(Li) detector as a function of distance was measured with ^{133}Ba and ^{228}Th sources fixed to the stopper in the same experimental geometry. From this measurement it followed that the efficiency of the detector as a function of source-detector distance could be described in good approximation by a R^{-2} dependence, with R the distance between the source and a point

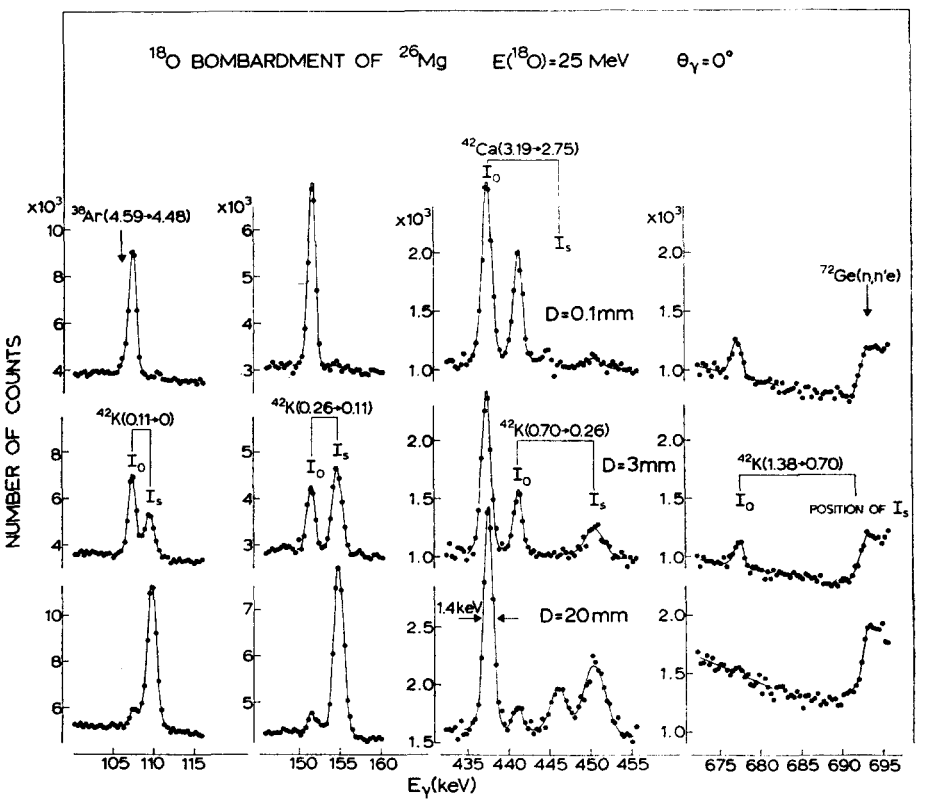

Fig. 5. Examples of the recoil-distance data obtained from the ^{26}Mg(^{18}O, pnγ)^{42}K reaction at different plunger distances D. The solid lines are fits to the data of Gaussians on a quadratic background. The energy of the ^{18}O ions after passage of the 1 μm Ni foil is 25 MeV.

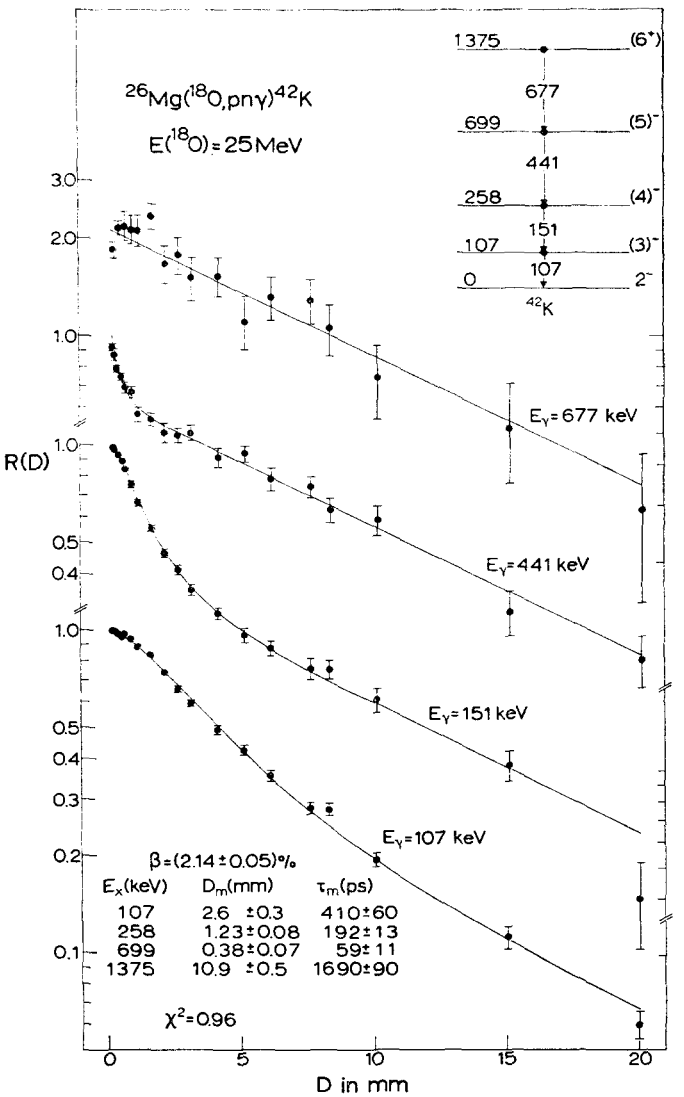

Fig. 6. The experimental ratios $R(D)$ as a function of the target-stopper distance D for the transitions shown in the decay scheme. The ratio $R(D)$ stands for $I_0/(I_0+I_s)$ except in the case of the 677 keV transition where $R(D)$ represents the ratio $A_0{}^{677}/A_0{}^{437}$ with $A_0{}^{677}$ the area of the stopped peak of the 677 keV transition and $A_0{}^{437}$ the area of the stopped peak of the ^{42}Ca(3.19 → 2.75 MeV) transition, corrected for the 7.79±0.13 ns lifetime of the 3.19 MeV level. The solid lines result from a simultaneous fit to all 72 data points, see subsect. 3.1.

inside the detector at 8 mm behind the front. The deviation from this description for γ-rays between 100 and 700 keV is less than 2% for the distances in the present experiment.

The shifted peak of the 677 keV γ-ray is obscured by the 692 keV structure from the ^{72}Ge(n, n'e) reaction (see fig. 5). Therefore the area of the stopped peak of the 677 keV transition is normalized by means of the area of the stopped peak of the 437 keV γ-ray transition, which originates from the 3.19 MeV level in ^{42}Ca. The small correction due to the 7.79 ± 0.13 ns mean life [5]) of ^{42}Ca(3.19 MeV) is taken into account. The resulting decay curve is the upper one shown in fig. 6.

In the decay curves of the $0.70 \rightarrow 0.26$, $0.26 \rightarrow 0.11$ and $0.11 \rightarrow 0$ MeV transitions in ^{42}K the sum of the stopped and the shifted peak of each γ-ray is used as normalization. The areas used for the construction of the $E_\gamma = 107$ keV decay curve were determined by fitting Gaussians superimposed on a quadratic background to the stopped and shifted peaks of the 107 and 106 keV γ-rays. The slight variation observed in the ratio of the areas $(106_0 + 106_s)/(107_0 + 107_s)$ is taken into account in the errors assigned to the extracted intensities of 107_0 and 107_s. The decay curves of the 677 and 441 keV γ-rays suggest that the long-lived component in the decay curve for the 441 keV γ-ray is due to feeding by the 677 keV γ-ray. Independent fits of these two curves give $D_m(677\text{ keV}) = 11.4 \pm 1.2$ mm and $D_m = 11.0 \pm 0.7$ mm for the longer component in the $E_\gamma = 441$ keV decay curve. In subsect. 3.2 it is shown that the 677 keV γ-ray indeed feeds the 0.70 MeV level.

In the $E_\gamma = 151$ keV decay curve three components are observed, the long-lived component corresponding to the lifetime of the 1.38 MeV level, the slight rounding at $D \lesssim 1$ mm due to the short lifetime of the 0.70 MeV level, and in between a component corresponding to the lifetime of the 0.26 MeV level. The composition of the $E_\gamma = 107$ keV decay curve is even more complex, but comparison with the decay curve of the 151 keV γ-ray indicates a lifetime for the 0.11 MeV level in between those for the 0.26 and 1.38 MeV levels.

The lifetimes of the four ^{42}K levels were finally obtained from a simultaneous fit of all four decay curves. The solid lines drawn in fig. 6 are the result of this fit. The expressions used are derived from the formulae for the sequential decay of up to four radioactive levels. In the fit to the 72 experimental data points, eleven parameters were adjusted, *viz.* the four characteristic distances, the feedings of the four levels and three normalization constants. The χ^2 of this simultaneous fit is 0.96.

In the results for the lifetimes given in the insert of fig. 6 only statistical errors are given. Because of possible deorientation effects 5 % is added[14]) quadratically to the

TABLE 2

Recoil-distance lifetime results for ^{42}K levels

E_x (MeV)	Transition (MeV)	τ_m (ps)	
		present	ref. [15])
0.11	$0.11 \rightarrow 0$	410 ± 60	370 ± 160
0.26	$0.26 \rightarrow 0.11$	192 ± 13	< 250
0.70	$0.70 \rightarrow 0.26$	59 ± 11	
1.38	$1.38 \rightarrow 0.70$	1690 ± 120	

statistical error in the lifetime of the 1.38 MeV level to give the final values listed in table 2. The previous value [15]) of $\tau_m = 360 \pm 160$ ps for the lifetime of ^{42}K(0.11 MeV) is consistent with the present result of $\tau_m = 410 \pm 60$ ps. Also the upper limit [15]) of $\tau_m < 250$ ps for the lifetime of ^{42}K(0.26 MeV) is in agreement with the value of $\tau_m = 192 \pm 13$ ps obtained in the present experiment. For the 0.70 and 1.38 MeV levels no previous values are known.

3.2. COINCIDENCE MEASUREMENTS BETWEEN DELAYED γ-RAYS

The position of the 677 keV γ-transition in the decay scheme given in fig. 6 has been established by means of a γ-γ coincidence experiment with the delayed set-up shown in fig. 7. Two Ge(Li) detectors with active volumes of 36 and 125 cm^3 were placed at $\theta_\gamma = 90°$. Gamma rays from the target were shielded with Ta and Pb so that only γ-rays from nuclei stopped in a Cu catcher placed 1.5 cm downstream ($\approx$ 2ns flight path) from the target could reach the detectors. The transmission from the target to the 36 cm^3 Ge(Li) detector was less than 2 % for $E_\gamma = 400$ keV, while the transmission from the catcher to the 36 cm^3 Ge(Li) was 85 % for $E_\gamma = 50$ keV and that from the catcher to the 125 cm^3 Ge(Li) detector 61 % for $E_\gamma = 150$ keV. With this set-up γ-rays originating from long-lived states are strongly enhanced.

Results of the γ-γ coincidence measurement with these delayed γ-rays are given in fig. 8, where spectra from the 36 cm^3 Ge(Li) detector are shown. The upper spectrum is coincident with γ-rays of an energy below 3 MeV in the 125 cm^3 detector, while the lower spectra are coincident with gates on ^{42}K transitions in the spectrum of the 125 cm^3 detector, as indicated. These latter coincidence spectra have been corrected for random coincidences and for the Compton background in the gates.

The 677 keV γ-ray is seen to be coincident with the 107, 151 and 441 keV γ-rays. For the intensity of any other γ-ray in coincidence with 677 keV an upper limit of 15 %

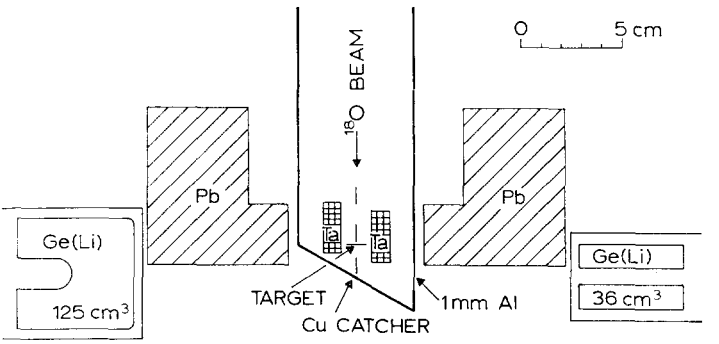

Fig. 7. Schematic view of the experimental set-up for the observation of delayed γ-rays. The target-catcher distance in the coincidence measurement was 1.5 cm, corresponding to a flight path of about 2 ns. The transmission for γ-radiation from the target to the 36 cm^3 Ge(Li) detector was less than 2 % for $E_\gamma = 400$ keV, while the transmission from the catcher to the 36 cm^3 detector was 85 % for $E_\gamma = 50$ keV and to the 125 cm^3 detector 61 % for $E_\gamma = 150$ keV.

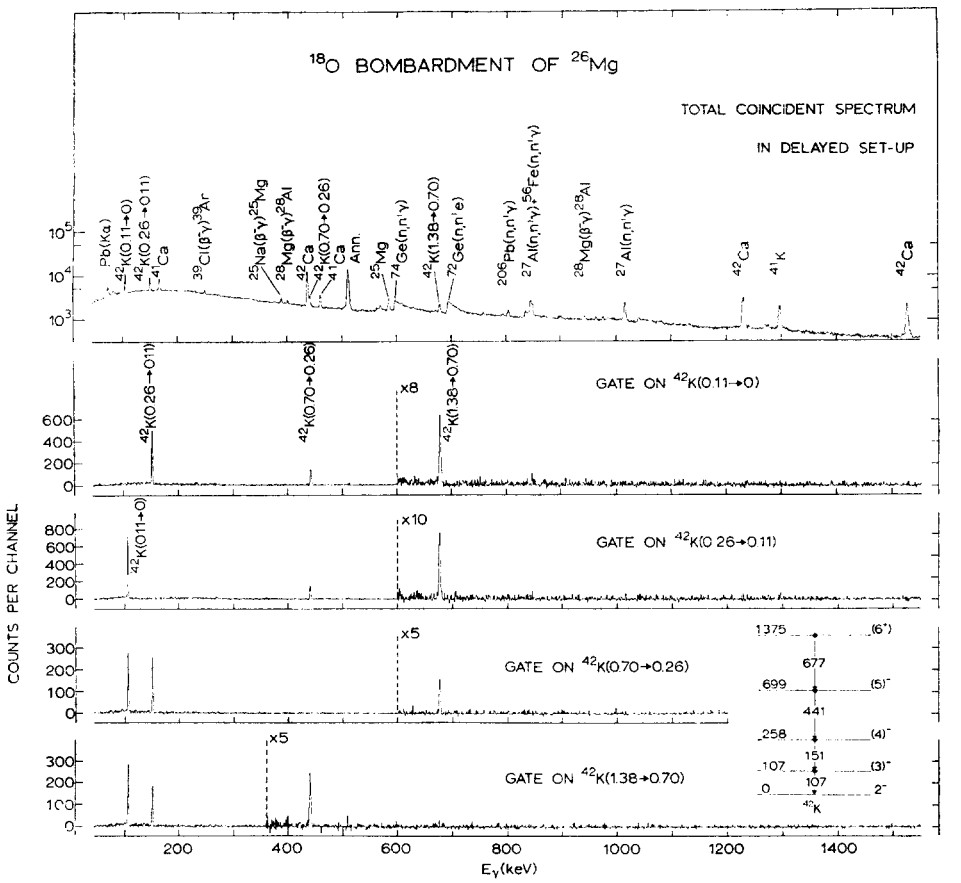

Fig. 8. Results of the γ-γ coincidence measurements with delayed γ-rays in the geometry of fig. 7. The total coincident spectrum of the 36 cm^3 Ge(Li) detector is shown on top. The lower spectra are coincident with the ^{42}K transitions in the spectrum of the 125 cm^3 Ge(Li) detector, as indicated. Background and random coincidences have been subtracted.

is given for the energy range 20–2000 keV. This upper limit is obtained from the coincidence spectra and for E_γ less than about 60 keV from the singles delayed γ-ray spectrum. In the latter spectrum only two γ-rays are observed between 20–60 keV, i.e. a 31 keV and a 53 keV γ-ray which are assigned to the ^{28}Mg(31 → 0 keV) and ^{73}Ge(67 → 13 keV) transitions, respectively.

From the presence of a 1.7 ns component in the decay curve of the 441 keV γ-ray in the recoil distance measurements (see fig. 6) it was already concluded that the 677 keV γ-ray originates from a ^{42}K level with $E_x \geqq 1375$ keV. Combination of the recoil-distance and γ-γ coincidence results establishes the existence of a ^{42}K level at an excitation energy of 1375.5 ± 0.2 keV with a mean life of $\tau_m = 1.69 \pm 0.12$ ns and exclusive decay to the $J^\pi = (5)^-$, 699 keV level (see subsect. 3.4).

3.3. EXCITATION ENERGIES

The energies of the ^{42}K transitions were determined from singles γ-ray spectra, taken in the set-up of fig. 7. Appropriate calibration lines from radioactive sources of ^{182}Ta [ref. [16])], ^{133}Ba [ref. [17])], ^{137}Cs [ref. [17])], and ^{228}Th [ref. [18])] were mixed with the spectra. Also the ^{181}Ta Coulomb excitation lines [19]) of 136.25±0.02 and 165.15±0.20 keV and the 460.27±0.10 keV ^{41}Ca(3.83 → 3.37 MeV) transition [20]) were used in the calibration.

The recoil-corrected γ-ray energies obtained for the four ^{42}K transitions are: 106.78±0.02, 151.33±0.12, 440.68±0.12 and 676.69±0.12 keV. The errors include statistical errors as well as uncertainties in the calibration energies. The resulting excitation energies are given in table 3.

The energies of ^{42}K γ-rays given by Warburton *et al.* [21]) are in good agreement with the results mentioned above, although the decay scheme is not discussed in ref. [21]).

TABLE 3

Excitation energies [a]) (in keV) of four ^{42}K levels

present work	Ref. [5])
106.78±0.02	107.2±0.3
258.11±0.12	258.5±0.5
698.79±0.17	700±2
1375.5±0.2 [b])	

[a]) As calculated from recoil corrected γ-ray energies.
[b]) New level.

3.4. UPPER LIMITS ON BRANCHING RATIOS

Upper limits (at the 95 % confidence level) for branching ratios of ^{42}K levels are given in table 4. They were mainly determined in a singles delayed γ-ray spectrum taken with the 36 cm^3 Ge(Li) detector in the set-up of fig. 7. In the cases where a

TABLE 4

Branching ratios [a]) (in %) for ^{42}K levels

From \ To	0	0.11	0.26	0.64	0.68	0.70	0.78	0.84	1.11	1.19	1.26
1.38	< 5	< 15	< 4	< 4	< 7	100	< 4	< 7	< 1.1	< 0.9	< 0.8
0.70	< 3	< 2.5	100	< 1.0							
0.26	< 1.5	100									
0.11	100										

The excitation energies E_x (MeV) are taken from ref. [5]) except for the 1.38 MeV level which is from the present work.

[a]) The upper limits are given at the 95 % confidence level and include a 30 % contribution to encompass possible angular distribution effects.

TABLE 5
Transition strengths

Nucleus	Transition (MeV)	$J_i^\pi \to J_f^\pi$ [a]	δ [a]	Branching [a] (%)	Transition strength (W.u.) [b]	
					M1	E2
^{21}Ne	0.35 → 0	$\frac{5}{2}^+ \to \frac{3}{2}^+$	0.03±0.03	100	0.056±0.007	
^{24}Na	0.56 → 0.47	$2^+ \to 1^+$	$\lvert\delta\rvert < 0.012$ [f]	97.5±0.5 [c]	0.88±0.11	
	0.56 → 0	$2^+ \to 4^+$		2.5±0.5 [c]		1.9±0.5
^{25}Mg	0.97 → 0.59	$\frac{3}{2}^+ \to \frac{1}{2}^+$	−0.12±0.03 [d]	49±2	0.015±0.001	8±4
	0.97 → 0	$\frac{3}{2}^+ \to \frac{5}{2}^+$	−0.34±0.09	51±2	$(9.2\pm0.8)\times10^{-4}$	0.7±0.3
^{42}K	0.11 → 0	$(1\text{–}3)^- \to 2^-$	$\lvert\delta\rvert < 0.08$ [f]	100	0.062±0.008 [e]	

[a]) Ref. [5]), unless indicated otherwise.
[b]) Calculated with the lifetimes from the present experiment (see tables 1 and 2).
[c]) Ref. [4]).
[d]) Ref. [6]).
[e]) Total conversion coefficient $\alpha_K = 0.018$, as extrapolated from the tables of Rose [24]) has been taken into account.
[f]) Calculated with the mean lives from the present experiment and a maximum E2 strength of 100 W.u. [ref. [29])].

possible transition was hidden under a contaminant peak the upper limit was obtained from the γ-γ coincidence measurement, described in subsect. 3.2. The upper limits given include a 30 % contribution to encompass possible angular distribution effects.

4. Discussion

4.1. TRANSITION STRENGTHS

The mean lives given in tables 1 and 2 lead to the transition strengths listed in table 5. A calculation with the wave functions of ref. [22]) yields for the 0.56 → 0.47 MeV, M1 transition in ^{24}Na a strength of 0.82 W.u., in excellent agreement with the experimental result of 0.88 ± 0.11 W.u. However, a recent calculation with the (in general) improved wave functions given in ref. [23]) results in an M1 strength of only 0.13 W.u. for the set of wave functions labeled ASDI and 0.90 W.u. for the MSDI set. In the calculations bare-nucleon g-factors are used.

The experimental M1 strength of the ^{42}K(0.11 → 0 MeV) transition can be deduced from the present data in spite of the fact that the spin of the initial level and the mixing ratio of the transition are unknown. Observation of $l_n = 1 + 3$ for this state in the ^{41}K(d, p)^{42}K reaction [5]) determines its parity as negative and limits the spin to 1, 2 or 3. The transition to the $J^\pi = 2^-$ ground state has therefore M1 as lowest multipolarity. Allowance of up to 100 W.u. E2 strength in this low-energy M1 transition limits the mixing ratio to $|\delta| < 0.08$, i.e. the E2 admixture is less than 0.7 % of the total intensity.

4.2. WEAK-COUPLING CALCULATION FOR $J^\pi = 6^+$ AND 7^+ STATES IN ^{42}K

In this section the binding energies of some particle-hole states in ^{42}K are calculated in the framework of the Bansal-French-Zamick weak-coupling method as used recently by Sherr *et al.* [25]) and Lawson [26]).

The binding energy of a particle-hole state with p particles and h holes and isospin T in the nucleus A, T_3 is given by

$$E(A, T, T_3) = E_h(h, T_h, T_{h3}) + E_p(p, T_p, T_{p3}) - hpa + \tfrac{1}{2}b\{T(T+1) - T_p(T_p+1) - T_h(T_h+1)\} + \tfrac{1}{4}c(p-2T_{p3})(h+2T_{h3}), \quad (2)$$

as follows from the formula given by Sherr *et al.*; E_p and E_h are the binding energies of the (excited) nuclei with p particles and h holes, respectively, of which the particle-hole state is composed. In this paper all binding energies are taken with respect to the ^{40}Ca ground state. The parameters a, b and c, are obtained from a least-squares fit [26]) to a number of particle-hole states in the ^{40}Ca region, which yields the values $a = -262$ keV, $b = 2549$ keV and $c = -337$ keV.

For the $J^+ = 6^+$ and 7^+ states in ^{42}K with the (stretched isospin) configurations $[(1d_{\frac{3}{2}}^{-2})_{01}(1f_{\frac{7}{2}}^{4})_{J1}]_{J^+,\,2}$, eq. (2) becomes

$$E[^{42}\mathrm{K}(J^+, 2)] = E[^{38}\mathrm{Ar}(0^+, 1)] + E[^{44}\mathrm{Sc}(J^+, 1)] - 8a + b + 2c.$$

The model therefore predicts the energy differences between the 6^+ and 7^+ states in ^{42}K and ^{44}Sc to be the same. The experimental excitation energies for ^{38}Ar(0^+, 1), ^{44}Sc(6^+, 1) and ^{44}Sc(7^+, 1) of 0, 0.27 and 0.97 MeV [refs. [27,28])], respectively, lead then in combination with the values for *a*, *b* and *c* given above to $E[^{42}\mathrm{K}(6^+, 2)] = -15.52$ MeV and $E[^{42}\mathrm{K}(7^+, 2)] = -14.83$ MeV.

The $[(1d_{\frac{3}{2}}^{-1})_{\frac{3}{2}\frac{1}{2}}(1f_{\frac{7}{2}}^{3})_{\frac{7}{2}\frac{3}{2}}]_{J^-,2}$ quadruplet with $J^\pi = 2^-, 3^-, 4^-$ and 5^- is degenerate in this weak-coupling model and is calculated at -16.74 MeV with respect to ^{40}Ca (g.s.). Experimentally, the $(2J+1)$ averaged center of gravity of the 2^-, $(3)^-$, $(4)^-$ and $(5)^-$ levels [5]) of ^{42}K at 0, 0.11, 0.26 and 0.70 MeV, respectively, has an energy of -16.76 MeV with respect to ^{40}Ca(g.s.).

The results mentioned above are summarized in fig. 9. The indicated experimental $J^\pi = (7^+)$ state at $E_x = 1.95 \pm 0.03$ MeV is taken from the ^{40}Ar(α, d)^{42}K work of Kouzes and Sherr [27]).

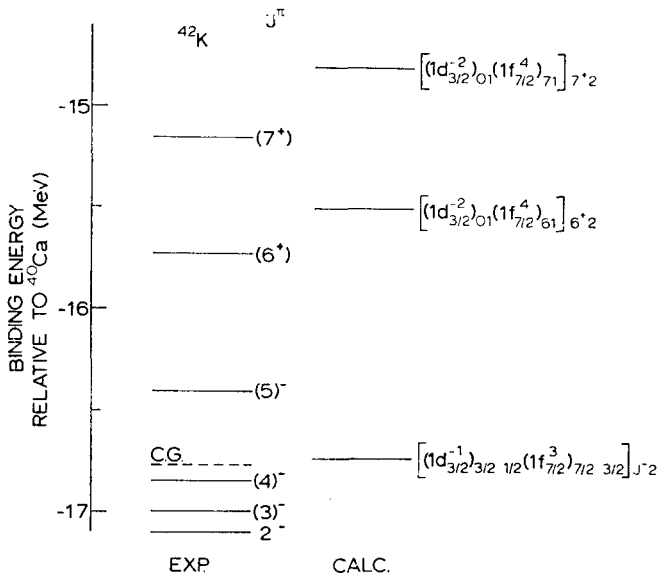

Fig. 9. Comparison of experimental and calculated binding energies for ^{42}K states. The energies are calculated in a weak-coupling model, see subsect. 4.2. The dotted line indicates the center of gravity of the (in this model degenerate) negative parity quadruplet.

Assignment of the $[(1d_{\frac{3}{2}}^{-2})_{01}(1f_{\frac{7}{2}}^{4})_{6+1}]_{6+,2}$ configuration to the long-lived level at 1.38 MeV would lead to a $6^+ \rightarrow 5^-$ E1 transition of 1.5×10^{-6} W.u. The large retardation would be consistent with the indicated main configurations, because a $f_{\frac{7}{2}} \rightarrow d_{\frac{3}{2}}$ dipole transition is forbidden.

Note added in proof: Recently Warburton *et al.* [30]) have assigned a 572.0+0.3 keV γ-ray to the decay of the (7^+) level at $E_x = 1.95$ MeV [ref. [27])] to the (6^+) level at

$E_x = 1.38$ MeV. An upper limit of $\tau_m(E_\gamma = 572 \text{ keV}) \leqq 750 \pm 200$ ps was obtained for this γ-ray in a RD experiment with the $^{27}Al + ^{18}O$ reaction. The data from the present experiment result in $\tau_m(E_\gamma = 572 \text{ keV}) \leqq 8$ ps.

One of us (L.P.E.) gratefully acknowledges the hospitality extended to him at the "Fysisch Laboratorium" and the financial support from the Swedish Atomic Research Council. This work was performed as part of the research programme of the "Stichting voor Fundamenteel Onderzoek der Materie" (FOM) with financial support from the "Nederlandse Organisatie voor Zuiver-Wetenschappelijk Onderzoek" (ZWO).

References

1) E. K. Warburton, *Proc. Int. Conf. on nuclear structure and spectroscopy, Amsterdam 1974, vol. 2*, ed. H. P. Blok and A. E. L. Dieperink (Scholar's Press, Amsterdam, 1974) p. 506
2) M. A. van Driel *et al.*, Nucl. Phys. **A226** (1974) 326
3) A. R. Poletti, B. A. Brown, D. B. Fossan and E. K. Warburton, Phys. Rev. **C10** (1974) 2312
4) A. S. Keverling Buisman and P. J. M. Smulders, Nucl. Phys. **A228** (1974) 205
5) P. M. Endt and C. van der Leun, Nucl. Phys. **A214** (1974) 1
6) P. A. Butler *et al.*, J. Phys., to be published
7) D. C. Bailey *et al.*, J. Phys. **A4** (1971) 908
8) R. J. Nickles, Nucl. Phys. **A134** (1969) 308
9) E. K. Warburton, J. W. Olness, G. A. P. Engelbertink and K. W. Jones, Phys. Rev. **C3** (1971) 2344
10) D. Schwalm, thesis, Heidelberg, 1969
11) R. A. Mendelson and R. T. Carpenter, Phys. Rev. **165** (1968) 1214
12) T. K. Alexander, O. Häusser, A. B. McDonald and G. T. Ewan, Can. J. Phys. **50** (1972) 2198
13) D. J. Donahue and R. L. Hershberger, Phys. Rev. **C4** (1971) 1693
14) N. Wüst *et al.*, J. Phys. **G1** (1975) 57
15) R. T. Carpenter and R. A. Mendelson, Bull. Am. Phys. Soc. **14** (1969) 585
16) W. Beer and J. Kern, Nucl. Instr. **117** (1974) 183
17) J. B. Marion, Nucl. Data **A4** (1968) 301
18) S. C. Pancholi and M. J. Martin, Nucl. Data Sheets **B8** (1972) 165
19) Y. A. Ellis, Nucl. Data Sheets **9** (1973) 319
20) P. Gorodetzky *et al.*, Phys. Rev. Lett. **31** (1973) 1067
21) E. K. Warburton *et al.*, At. Data and Nucl. Data Tables **14** (1974) 147
22) J. F. A. van Hienen, P. W. M. Glaudemans and J. van Lidth de Jeude, Nucl. Phys. **A225** (1974) 119
23) F. Meurders, P. W. M. Glaudemans, J. F. A. van Hienen and G. A. Timmer, Nucl. Phys., to be published
24) M. E. Rose, *Internal conversion coefficients* (North-Holland, Amsterdam, 1958)
25) R. Sherr, R. Kouzes and R. Del Vecchio, Phys. Lett. **52B** (1974) 401
26) R. D. Lawson, Argonne Nat. Lab., private communication
27) R. Kouzes and R. Sherr, Bull. Am. Phys. Soc. **18** (1973) 602, and private communication
28) J. J. Kolata, J. W. Olness and E. K. Warburton, Phys. Rev. **C10** (1974) 1663
29) P. M. Endt and C. van der Leun, Nucl. Phys. **A235** (1974) 27
30) E. K. Warburton, J. J. Kolata and J. W. Olness, Phys. Rev. **C11** (1975) 700